Recognition of dominant driving factors behind sap flow of Liquidambar formosana based on back-propagation neural network method

Jie Tu, Qijing Liu, Jianping Wu

Annals of Forest Science (2021) 78: 95
https://doi.org/10.1007/s13595-021-01091-y

RESEARCH PAPER

Recognition of dominant driving factors behind sap flow of *Liquidambar formosana* based on back-propagation neural network method

Jie Tu[1] · Qijing Liu[2] · Jianping Wu[3]

Received: 31 July 2020 / Accepted: 27 July 2021 / Published online: 12 November 2021

Abstract

Key message **Three-layered back-propagation (BP) neural networks with architecture 4–10-1 (four neurons in the input layer, ten neurons in the hidden layer and one neuron in the output layer) performed better than MLR (multivariate linear regression) in modelling complex nonlinear relationships between sap flow and driving factors. The optimum BP model was achieved with an input combination of air temperature, relative humidity, average net radiation, and a phenological index. The performance of BP models indicated a small improvement with the inclusion of a phenological index.**

Aims This study focused on the applicability of back-propagation (BP) neural networks in simulating sap flow (SF) using meteorological factors and a phenological index (*PI*) for *Liquidambar formosana*, a deciduous broad-leaf tree species in subtropical China, and thus providing a useful and promising alternative to traditional methods for transpiration prediction.

Methods Three-layered BP models with an architecture 4–10-1 (four neurons in the input layer, ten neurons in the hidden layer and one neuron in the output layer) were trained and tested using the Levenberg–Marquardt (LM) algorithm based on in situ observations of SF and concurrent microclimate at the Qianyanzhou Ecological Station, Jiangxi Province, Southeast China. The model performance was verified with testing data not used in model development.

Results The BP models with eight input combinations proved a satisfactory fit: the determination coefficients (R^2) and fitting accuracies (*Acc*) (about 0.8 and 70%) were significantly higher than those of the multivariate linear regression (MLR) (about 0.5 and 50%), indicating their advantage in solving complex nonlinear relationships involved in transpiration. In addition, the BP models showed a bit better performance by adding *PI* to the input family. The best BP model was achieved taking air temperature (T_a), relative humidity (*RH*), average net radiation (*ANR*), and *PI* as the input and sap flux density (v_s) as the output, with maximum R^2 and *Acc* as high as 0.95 and 90%, respectively.

Conclusion The BP models with input combination of T_a, *RH*, *ANR*, and *PI* mirrored very well measured daily variations in v_s. The results could be used to fine-tune estimations of sap flow by *Liquidambar formosana*, and thus shed light on the eco-hydrological process related to transpiration for deciduous broad-leaf trees.

Keywords *Liquidambar formosana* · Sap flux density · Meteorological factors · Back-propagation neural network · Phenological index

1 Introduction

Transpiration contributes a lot to the hydrologic cycle in forest ecosystems (Deutscher et al. 2016; Fatichi and Pappas 2017; Wilson et al. 2001) and reflects the photosynthetic activity of plants to the changing climatic conditions (Evaristo et al. 2016; Grossiord et al. 2017). Thus, the study of transpiration and its environmental sensitivity is of importance to understand water cycling and tree physiology (Bauerle et al. 2002; Konings et al. 2017). In the past decades, a few techniques have been developed to measure transpiration, including gas

Handling Editor: Barry A. Gardiner

Contribution of the co-authors JT acquired funding and designed the experiment. QL and JW collected and analyzed the data. The authors jointly contributed to manuscript completion.

✉ Jie Tu
tujie8058@163.com

Extended author information available on the last page of the article

exchange systems (e.g., Monje et al. 2000; Dragoni et al. 2005), micrometeorological techniques (e.g., Aouade et al. 2016; Saugier et al. 1997), and chemical tracers (e.g., Calder et al. 1986). However, there are major drawbacks associated with these techniques (González-Altozano et al. 2008; Kalma et al. 1998). In addition, numerous modelling approaches have also been applied to predict transpiration with relevant driving parameters, such as semi-empirical models (Monteith 1997; Paudel et al. 2015) and empirical models (Buckley et al. 2012; Whitley et al. 2013). Unfortunately, these models failed to yield satisfactory results because most of them required extensive data inputs that are not included in conventional observations (Fernandes et al. 2015; Gharun et al. 2015) or needed special parameterization unavailable for different species (Buckley et al. 2012). Furthermore, these methods often underestimate nighttime transpiration, an essential part of plant water consumption (Cavender-Bares et al. 2007; Moore et al. 2008).

The sap flow (SF) method using heat as a tracer has been routinely used for continuous measurements of plant water consumption with high-precision and mild impact across spatiotemporal scales (Dragoni et al. 2005; Kallarackal et al. 2013). Currently, several advanced methods are available to measure sap flow (Vandegehuchte and Steppe 2013). Nonetheless, efforts remain in optimizing the existing methods and developing new approaches (Vandegehuchte et al. 2015; Windt and Blümler 2015). The SF method also allowed researchers to make inferences about water status (Venturin et al. 2020), plant water relations to the environment (Miner et al. 2017; Paudel et al. 2015) and the impact of changing climate (Berdanier and Clark 2018) and forest management practices (Fernandes et al. 2015; Han et al. 2019) in forested landscapes. It is well acknowledged that sap flow is controlled not only by meteorological parameters such as temperature (T_a), vapor pressure deficit (*VPD*) (Hayat et al. 2020; Juhász et al. 2013; Pfautsch et al. 2010), and soil water content (Nadal-Sala et al. 2017) but also by physiological parameters such as LAI (Liu et al. 2009; Navarro et al. 2018; Tu et al. 2019). Obvious differences exist between the response of SF and its sensitivity to meteorological factors under different soil water conditions (Chen et al. 2014; Hayat et al. 2020). The interactions between those parameters are complex, and many of them are typically highly correlated (Asbjornsen et al. 2011). Many traditional models combining environmental factors with physiological factors have been used to acquire more-accurate estimates of SF (Chen et al. 2014; Liu et al. 2017; Tie et al. 2017). Nevertheless, these models worked unsatisfactorily with poor accuracy because of their basic assumption on the normal distributions of the data set and linear relationships between input and output. Hence, a novel technique capable of mapping the complex non-linear process involved in transpiration is necessary.

Due to its advantages of self-organization, self-learning, and self-adapting (Faris et al. 2019), the artificial neural network (ANN) was proposed as an efficient and useful modelling approach to identify the implicit input–output relationships to an arbitrary degree of accuracy without specifying the underlying complex nature in an explicit mathematical form (Adeloye et al. 2012; Nourani et al. 2011). In the past decades, ANN has been intensively applied for resolving complex problems in the fields of forest and agriculture hydrology, e.g., evapotranspiration (Abrishami et al. 2019), trunk sap flow (Gharun et al. 2015), and transpiration (Garcia-Santos 2011; Xu et al. 2017). The back-propagation (BP) neural network is one of the most commonly used types, owing to its ability to approach a discretionary nonlinear function with good fitting results without any restrictive assumptions about the functional form of the underlying process (Humphrey et al. 2016; Nourani and Kalantari 2010). Many researchers have found better performance of BP neural networks over traditional models in modelling sap flow or transpiration (Fernandes et al. 2015; Gharun et al. 2015; Xu et al. 2017), but our understanding of time-lag effect or phenological influence on neural networks is still limited in various species (Chen et al. 2020; Tu et al. 2019).

Based on the in situ observations of SF and microclimate on a *Liquidambar formosana* plantation from April to December in 2014, a three-layered BP neural network with the architecture 4–10-1 was constructed to describe the complex nonlinear relationships between SF, meteorological factors, and phenological index (PI). Specifically, we intended to (1) detect the dominant driving factors controlling sap flow with a single-variable analysis method, (2) identify the advantages of BP models in mapping the complex non-linear correlations between SF and its driving factors using multivariate linear regression (MLR) as a benchmark, and (3) evaluate the performance of BP models retrieved by various input combinations and determine the most relevant inputs affecting SF. This study examines the utility of BP methods in modelling SF of *Liquidambar formosana* with the minimum input variables of climatic data and physiological factor, which is complementary to our previous paper that reported results for *Pinus massoniana* (Tu et al. 2019). The results will also be helpful for proving the fact that the methodology works for both a gymnosperm and an angiosperm.

2 Materials and methods

2.1 Study site

This research was conducted in the Qianyanzhou Ecological Station (115° 04′ 13″ E, 26° 44′ 48″ N; 102 m a.s.l.), affiliated with the Institute of Geographic Sciences and Natural Resources Research, Chinese Academy of Science, located

in Taihe County of Jiangxi Province, Southeast China. It is characteristic of a typical subtropical monsoon climate with high temperatures and abundant precipitation. The annual accumulative sunshine hours is 1360 h with gross radiation intensity reaching 4349 MJ·m^{-2}. The annual average temperature is 17.8 °C with the maximum monthly average temperature being 28.8 °C in July and the minimum of 6.4 °C in January. Although the annual mean rainfall reaches 1500 mm, more than 50% is concentrated between April and June with less in the summertime, and is unequally distributed among the four seasons of a year. The dominant soil is a red Oxisol according to FAO classification, developed from slate and shale (Wang et al. 2008). Sample plot investigation was conducted on a mixed broadleaf-conifer forest (*Liquidambar formosana*, *Cunninghamia lanceolate*, *Pinus massoniana*, *Schima superba*) in 2014. The stand density was 2280 stems·ha^{-1} with the average DBH and height of *Liquidambar formosana* being 20.5 cm and 15.7 m, respectively. The canopy cover is as high as 0.9 in the sample plots, with a few shrubs of *Symplocos sumunti* and herbs of *Dalbergia hupeana* sparsely distributed in the understorey.

2.2 Measurement of sap flow and environmental variables

Sap flux density (v_s, cm^3·cm^{-2}·s^{-1}) was continuously measured on nine sample trees (three in each plot) using thermal dissipation probes (TDP-30, Dynamax Inc., Houston, TX, USA) from April 2014 to December 2014. The DBH of sample trees ranged between 20.6 and 21.8 cm, averaging around 21.2 cm. A probe set consists of two parts: the heating needle installed above using a resistance wire to provide constant heating; the reference needle installed below without heating. The installation of the probes followed procedures recommended by the manufacturer. All probes were mounted on the northern side of the trunk at 1.5 m height above the ground and wrapped with aluminium-foil paper to avoid physical trauma and thermal effects from solar radiation. The data were recorded at 60 s intervals and stored as 30 min averages on a data logger (DT-50, Thermo Fisher Scientific Inc., Waltham, USA). Sap flux density (v_s) was calculated based on the empirical relationship established by Granier (1987)as *Eq.* 1:

$$v = 0.0119 \times \left(\frac{\Delta T_{max} - \Delta T}{\Delta T} \right)^{1.231} \quad (1)$$

where ΔT is the temperature difference between the thermal needle and the reference needle, ΔT_{max} is the maximum ΔT recorded during the period of nearly no sap flow, often occurring at predawn (Rabbel et al. 2016).

Air temperature (T_a), relative humidity (*RH*), wind velocity (W_s), and average net radiation (*ANR*) were synchronously monitored by the routine meteorological instruments (Model HMP 45C, Vaisala Inc., Finland) at 15 m on the flux tower, which was about 200 m away from the study plot. Soil moisture (θ) at a depth of 10 cm was obtained by a soil moisture sensor (Model CS616, Campbell Scientific Inc., USA). All data were recorded at 60 s intervals and stored as 30 min averages on a data logger (Model CR1000, Campbell Scientific Inc., USA). The dynamic responses of SF to meteorological factors were assessed using a cross-correlation analysis. A range of time-lags were introduced for each pair of time series, and the corresponding range of correlation coefficient (r) was obtained by using the cross-correlation function (Oguntunde et al. 2004). The lag that corresponds to maximum r is retained as the time-lag for that pair. In this study, sap flow lagged behind *ANR* by about 60 min, whereas no time shift was detected between SF and T_a and *RH*. All data sets have been deposited into the Dryad repository (Tu et al. 2021).

2.3 Data pre-processing

Data pre-processing can make ANN model training more efficient, including input variables selection, outlier exclusion, data division, and normalization. A single-variable analysis was performed on related driving factors affecting sap flow (i.e., T_a, *RH*, W_s, *ANR*, and θ). Additionally, the phenological index (*PI*), a kind of time factor with a specific value assigned for any sampling time, was introduced to characterize the phenological influence on SF (Tu et al. 2019). Following the method suggested by Li et al. (2006), we obtained a total of 10,800 groups of data set by eliminating abnormal ones. The total data set were randomly split into two groups with the coin flipping method. All the original data set were normalized by a hyperbolic tangent function and transformed into the range of [0,1]. More details about input variables selection, outlier exclusion, data division, and normalization can be found in the previous study (Tu et al. 2019).

2.4 Backpropagation neural network modelling

A three-layer feed-forward back-propagation (BP) neural network was used to simulate sap flux density (v_s) using a commercial software package (MATLAB, The MathWorks Inc., Natwick, MA, 2014). Meteorological parameters and the *PI* were selected as the input variables, and v_s as the output. The training process repeated until a minimum acceptable error (0.0001) was achieved between the measured and target output values (Eq. 2). After about 2000 iterations, the optimum BP architecture 4–10-1 (four neurons in the input layer, ten neurons in the hidden layer and one neuron in the

output layer) was identified through comparisons of different network structures by cross-validation and adjusting the network parameters. More details about BP neural network modelling can be found in the earlier paper (Tu et al. 2019).

$$E = \frac{1}{2}\sum_{p}\left(t_i - a_i\right)^2 \quad (2)$$

where t_i is the target output for the ith pattern, a_i is the measured output for the ith pattern.

2.5 Model evaluation

The two statistical parameters, coefficients of determination (R^2) and fitting accuracy (Acc), were used to assess the performance of BP neural network and MLR by comparing the measured and target values of v_s (Tu et al. 2019).

3 Results

3.1 Multiple linear regression analysis

According to the single-variable analysis between input and output variables, sap flux density (v_s) correlated positively with air temperature (T_a) and average net radiation (ANR) ($p < 0.001$), but negatively with relative humidity (RH) ($p < 0.001$), with correlation coefficients of 0.438, 0.619, and − 0.323, respectively (Table 1). The sequence for meteorological factors affecting the accuracy of the model was $ANR > T_a > RH$, indicating that the contribution of solar radiation to SF was greater than T_a and RH. However, other variables, such as wind speed (W_s) and soil moisture (θ), did not significantly contribute to explaining SF and indicated no significant correlations ($p > 0.05$) with SF.

To identify the superiority of BP methods over traditional statistical models in mapping complex nonlinear input–output relationships, multiple linear regression (MLR) equations were developed between v_s and the above three meteorological factors (with and without time-lag considered), with the confidence level of 95% to select and reduce dependent variables. The optimum MLR was achieved using the training data set (considering a time-lag effect), with the determination coefficient (R^2) and fitting accuracy (Acc) of 0.52 and 50%, respectively (Eq. 3). The value of R^2 indicated that 52% of the daily variation in SF could be explained by the combination of ANR and RH. Then, the optimum MLR was also validated using testing data set, with an R^2 and Acc of 0.51 and 50%, respectively. To sum up, the fitting performance derived from MLR was relatively poor, indicating that the complex relationships between SF and its driving factors are not well explained by the statistical regression analysis method.

$$v_s = 0.001 - 3.474 \times 10^{-5} RH + 4.774 \times 10^{-6} ANR \quad \left(R^2 = 0.52\ p < 0.001\ \mathrm{n} = 3000\right) \quad (3)$$

Table 1 Single-variable analysis between SF and its relevant variables

	T_a	W_s	ANR	RH	θ
v_s	0.438**	0.085	0.619**	-0.323**	0.018

**Indicates significant correlation at $p < 0.001$. v_s sap flow density ($cm^3 \cdot cm^{-2} \cdot s^{-1}$), T_a air temperature (°C), W_s wind speed ($m \cdot s^{-1}$), ANR average net radiation ($w \cdot m^{-2}$), RH relative humidity, θ soil moisture ($cm^3 \cdot cm^{-3}$)

3.2 Dependence of BP models on different input variables

On the basis of the training data set, eight BP models with the architecture of 4–10-1 were formulated to simulate SF by varying input variables, so as to determine the optimum BP model. The eight groups of input variables were selected as:

- Scheme 1: T_a and RH;
- Scheme 2: T_a and ANR;
- Scheme 3: RH and ANR;
- Scheme 4: T_a, RH, and ANR;
- Scheme 5: T_a, ANR, RH, and W_s;
- Scheme 6: T_a, RH, ANR, and PI;
- Scheme 7: T_a, RH, and ANR (considering time-lag effect);
- Scheme 8: T_a, RH, ANR (considering time-lag effect), and PI

In order to testify the feasibility of BP models in mapping the nonlinear relationships between SF and its driving factors, we randomly picked out 100 groups from the training data set to depict the line plots of the measured and simulated v_s by the eight input combinations (Fig. 1a–h denotes the measured and simulated v_s by BP models on scheme 1 ~ 8, respectively.)

As shown in Fig. 1, the simulated v_s by BP models matched well with the measured values, indicating that the BP models could satisfactorily describe the relationships between the input and output parameters during the training stage. Besides, the generalization ability of BP models was also validated using the testing data set with cross-validation analysis. It can be seen that all data points were well aggregated along the ideal unity-slope line (Fig. 2). Taken together, the

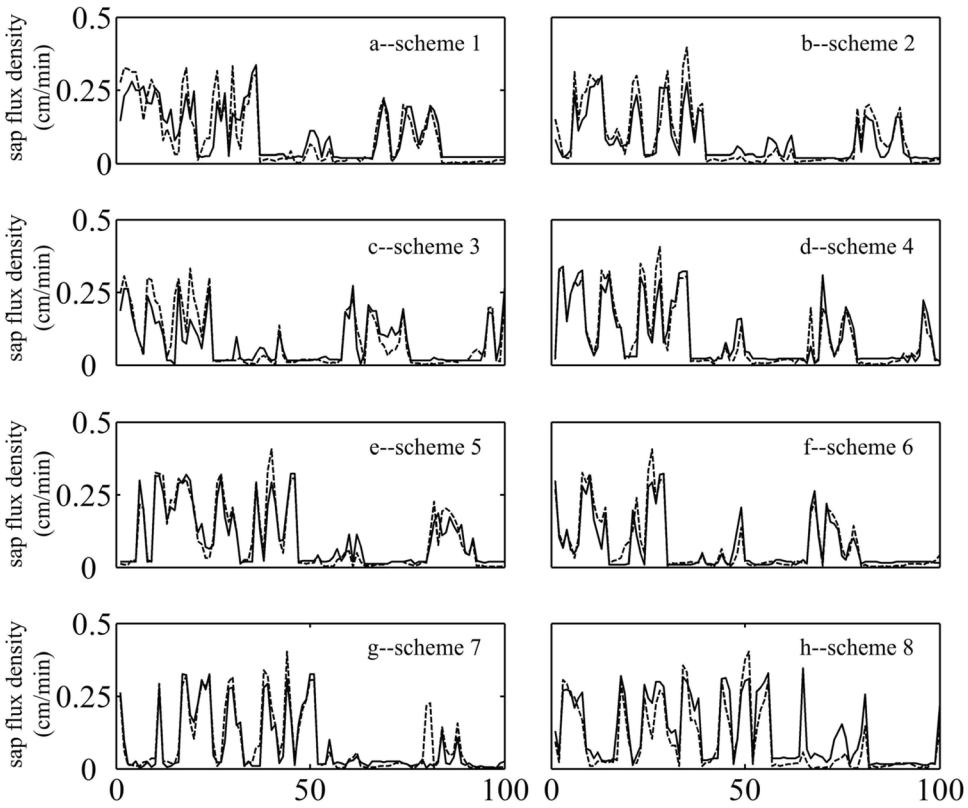

Fig. 1 Comparison of the measured and simulated sap flux density by BP neural networks with eight different combinations of input variables. (Each comparison uses a different set of measurement data. The dashed lines denote the measured values and the solid lines denote the target outputs)

BP models produced better fittings of SF compared to the MLR model, as reflected by the higher R^2 and *Acc* values of the eight models, fluctuating within the range of 0.80 ~ 0.95 and 72 ~ 90%, respectively (Fig. 2, Table 2).

However, it is noteworthy to mention that various results could come out in multiple trial experiments owing to random initialization of the weight vectors of neural networks, thus resulting in failure to obtain the optimum BP model. Therefore, we carried out 100 repeated trial experiments to test the sensitivity of BP models to different input variables (Fig. 3). Firstly, the minimum R^2 and *Acc* of 0.80 and 70% occurred with scheme 3 without T_a (Fig. 2c, Table 2), suggesting that the variable T_a was a crucial variable for SF simulation. Secondly, the R^2 and *Acc* were over 0.9 and 80% (Fig. 2d, e, f, g, h, Table 2) with T_a, *RH*, and *ANR* simultaneously included.

This supported the conclusions from the earlier multiple linear regression analysis that *ANR*, T_a, and *RH* were the dominant driving factors controlling SF in our study. The R^2 and *Acc* showed no significant increase when W_s was added to the BP models (Figs. 2e and 3, and Table 2), indicating that W_s was not a crucial variable controlling SF. Thirdly, the inclusion of phenological index (*PI*) related to physiological factors slightly improved the model performances (Figs. 2f and 3, Table 2).

Conversely, the inclusion of a time-lag effect did not significantly improve the performance of BP models (Figs. 2e and 3, Table 1), although there existed an approximately 60 min delay between SF and and *ANR*. Therefore, the optimum BP model was achieved by taking T_a, *RH*, *ANR*, and *PI* as the input variables, with a maximum R^2 and *Acc* of 0.95 and 90%, respectively.

4 Discussion

4.1 Dependence of sap flow on meteorological factors

Previous studies have indicated that *VPD*, solar radiation, and T_a are the most important environmental factors controlling sap flow, especially *VPD* and solar radiation (e.g., Chang et al. 2014; Chen et al. 2014; Liu et al. 2012; Tie et al. 2017). In our study, sap flow was tightly controlled by *ANR*, *RH*, and T_a. The correlation of sap flow to *ANR* was stronger than that with *RH* and T_a, and it explained 62% of the variation in SF (Table 1). This finding was consistent with the studies conducted in various species including *Populus davidiana*, *Albizia kalkora*, and *Acacia auriculiformis* (Tie et al. 2017; Wang et al. 2017). However, *VPD* contributed more to the variations in SF than solar radiation for *Pinus massoniana* in our eariler paper

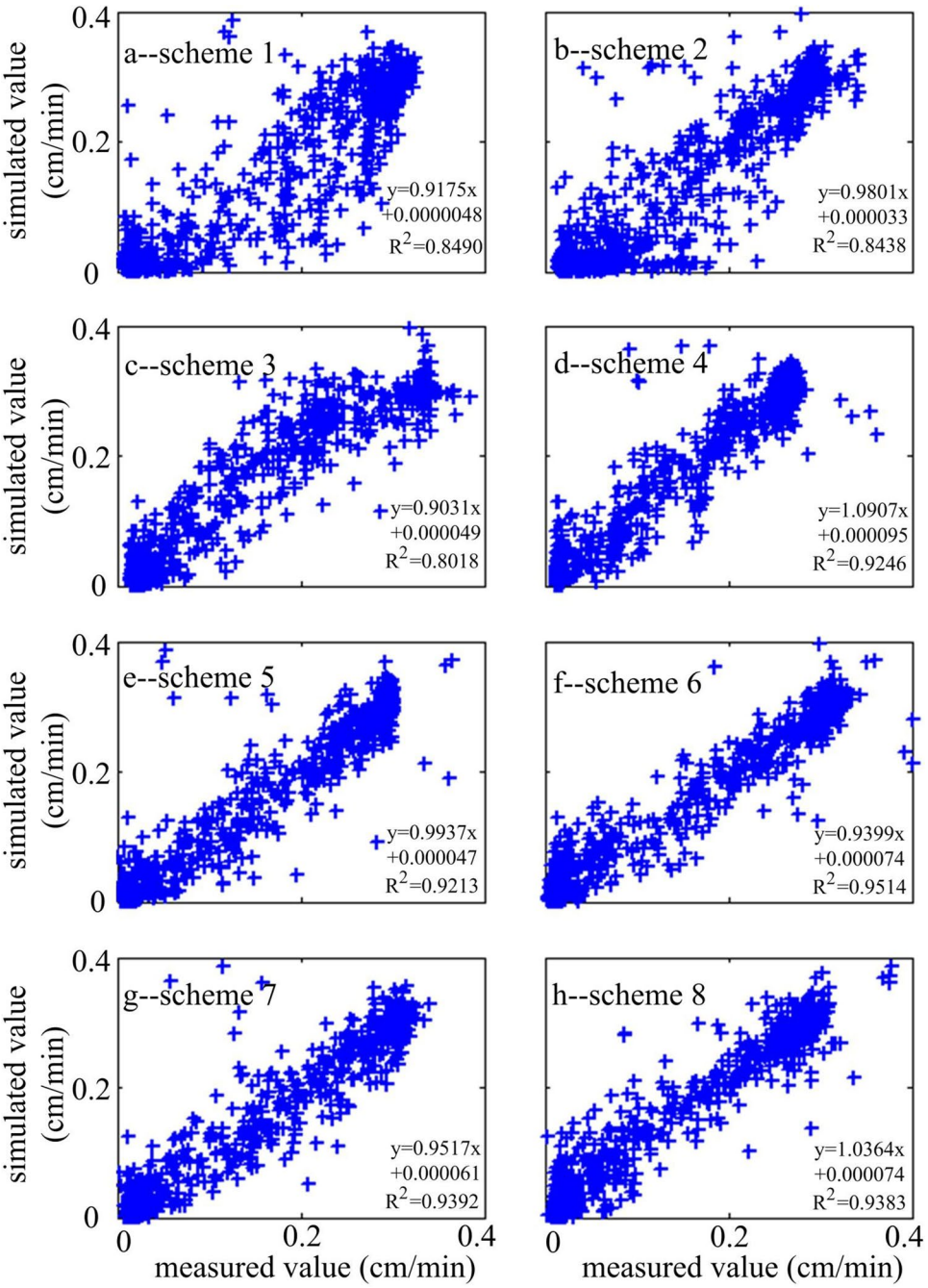

Fig. 2 Scatter plot between measured and simulated values of sap flux density using BP models based on eight combinations of input variables during the testing stage

Table 2 Fitting accuracy statistics of training and testing datasets from eight schemes

Data type		Scheme 1	Scheme 2	Scheme 3	Scheme 4	Scheme 5	Scheme 6	Scheme 7	Scheme 8
Max Acc	Training	0.8165	0.8173	0.7946	0.8877	0.8948	0.8983	0.9019	0.9032
	Testing	0.7954	0.7830	0.7443	0.8636	0.8680	0.8657	0.8929	0.8956
Min Acc	Training	0.7679	0.7808	0.7488	0.8596	0.8533	0.8752	0.8752	0.8644
	Testing	0.7470	0.7321	0.7038	0.8041	0.8025	0.8673	0.8370	0.8289
Med Acc	Training	0.776	0.8034	0.7698	0.8799	0.8817	0.8886	0.8731	0.8894
	Testing	0.7633	0.7810	0.7218	0.8655	0.8306	0.8667	0.8278	0.8321
Ave Acc	Training	0.7618	0.8027	0.7687	0.8765	0.8794	0.8830	0.8788	0.8843
	Testing	0.7650	0.7880	0.7209	0.8519	0.8251	0.8417	0.8231	0.8299

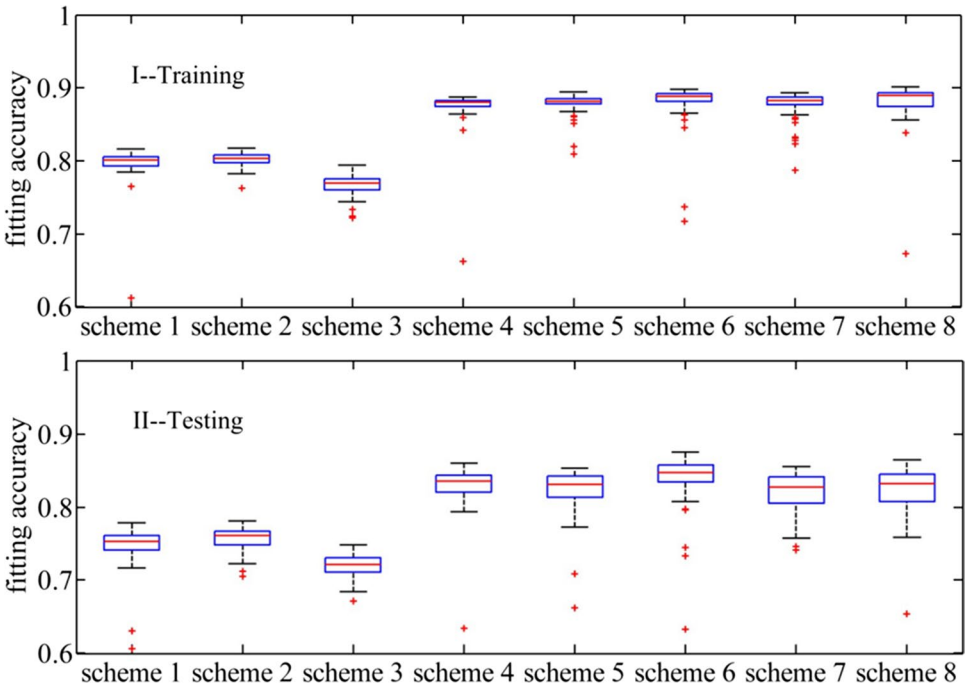

Fig. 3 Statistical analysis of fitting accuracies from eight BP neural networks. (I: denotes the *Acc* of the training datasets, and II: denotes the *Acc* of the testing datasets)

(Tu et al. 2019). This may be related to the differences in stomatal resistance. Moreover, the influences of environmental factors on SF vary with tree species, growth status, hydro-climatic characteristics, timescales, etc. (Chen et al. 2014; Du et al. 2011; Liu et al. 2012). Over short timescales (e.g., diurnally), solar radiation and *VPD* have been shown to exert more control on transpiration (Zha et al. 2017). However, over longer timescales (e.g., seasonally), available soil water and leaf phenology are more important (Hayat et al. 2020).

Many studies conducted in arid and semi-arid regions have concluded positive correlations between SF and soil moisture (Chang et al. 2014; Chen et al. 2014; Nadal-Sala et al. 2017; Telander et al. 2015), usually fitted by logistic regression (Chang et al. 2014) or exponential regression (Wu et al. 2018). Our result showed that there was poor correlation between SF and soil water content (θ), suggesting that the forest might not have been under any soil water stress during the experimental periods. This is consistent with the result from *Q. acutissima* and *C. lanceolata* in the Yangtze River Delta Region of China (Liu et al. 2017). The reason may be to do with the high soil moisture content derived from high annual rainfall (approximately 1500 mm). Furthermore, the relationship between SF and θ is complex (Brito et al. 2015). Plants adjust their structural or physiological characteristics to maintain the integrity of the hydraulic system under water stress (Bréda et al. 2006); thus, soil moisture reduction gave rise to a more significant effect on SF for shallow-rooted or less drought-sensitive species (McCarthy and Pataki, 2010; Zapater et al. 2011). However, others failed to confirm the restrictions of soil moisture on SF, particularly for deep root plants capable of accessing groundwater (Liu et al. 2017; Prieto et al. 2010). Therefore, a more clear and in-depth analysis of the relationship between SF and θ is needed to elucidate the effect of soil moisture on tree transpiration (Ghimire et al. 2014).

Wind speed (W_s) has been recognized as an important factor influencing tree transpiration (McNaughton and Jarvis 1983), which determines leaf boundary layer conductance and therefore modifies the rate of transport of water away from leaves (Kume et al. 2015). Significant positive correlations have been found between SF and W_s in *Salix psammophila* and *Larix principis-rupprechtii* (Huang et al. 2015; Han et al. 2019). However, Dixon and Grace (1984) predicted a negative response of transpiration to increasing W_s. A wind tunnel experiment on five tree species also suggested that the aerodynamic controls of tree transpiration by W_s probably results from differences in stomatal conductance rather than leaf type (Kume et al. 2015). In our study, no significant correlation was found between SF and W_s. The reason may be that a smaller stomatal conductance (g_s) relative to aerodynamic conductance (g_a) controlled the water movement between the leaf surface and atmosphere, leading to insignificant aerodynamic control on transpiration (Kume et al. 2015).

4.2 Dependence of sap flow on physiological factors

Significant difference can occur in sap flow dynamics even under similar weather conditions, probably attributable to growth differences at different phenological stages (Chirino et al. 2011; Fernandes et al. 2015; Tu et al. 2019). Phenology is a key

indicator describing the timing of certain periodical development stages of species throughout the year (Hudson 2010) and remains one of the most challenging processes to parameterize in ecosystem process models (Gonsamo et al. 2013). Therefore, it is important to consider phenology in modelling sap flow. As a vital index related to plant phenology, LAI is often used together with environmental factors for optimizing SF simulation (Obrist et al. 2003; Chang et al. 2014; Tie et al. 2017). However, LAI is only available at coarse spatial and temporal resolution (Bréda and Granier 1996; Garrity et al. 2011; Hayat et al. 2020). Thus, phenological index (*PI*) was used here to represent the impact of phenology on SF. Because climate data are well represented in the modelling, we believe that such an index can quantitatively capture the phenological influence when modelling SF. Based on the results above, we also found that the performance of BP models was only slightly improved by including *PI*, which is different from our previous result on *Pinus massoniana* (Tu et al. 2019), which showed a larger improvement. This low sensitivity of sap flow to phenology may be associated with the leaf emergence of *Liquidambar formosana*.

4.3 Time-lag between SF and meteorological factors

Time-lag between SF and meteorological factors has long been recognized in various ecosystems, species or geographical regions (Hayat et al. 2020; Zhang et al. 2019). The magnitude of the time-lag is dependent on biotic and abiotic factors and varies among species and seasons (Kume et al. 2008; Zhang et al. 2019). Among them, solar radiation and soil moisture were the prominent factors influencing diurnal time-lag loops (O'Grady et al. 2008; Tie et al. 2017). Under low radiation and soil water condition, the time-lag was significantly reduced (Hayat et al. 2020; Tie et al. 2017). Generally, sap flow is delayed relative to solar radiation but changes ahead of T_a and *RH* changes (Wang et al. 2017; Zhang et al. 2019). However, sap flow of *Salix psammophila* changes ahead of solar radiation (Hayat et al. 2020). Moreover, no time-lag was found between SF and *RH* for *Larix gmelinii* in the northeastern of China (Wang et al. 2011). In our study, sap flow only lagged behind *ANR* by 60 min, whereas no evident time-lag existed between SF and T_a and *RH*, which is not consistent with other studies (Hayat et al. 2020; Zhang et al. 2019). The performance of BP neural networks showed no significant improvement with time-lag included, which is not consistent with a previous study on the coniferous species *Pinus massoniana* (Tu et al. 2019).

5 Conclusions

Facing the complex hydrological and physiological process related to transpiration, this paper assessed the feasibility of BP neural networks in simulating the non-linear relationships between SF of *Liquidambar formosana* and its driving factors. The BP models outperformed the conventional method of MLR in simulating SF with high fitting accuracy and generalization ability, slightly improved by including a phenological index (*PI*). Therefore, the best BP neural network structure was achieved according to coefficients of determination (R^2) and fitting accuracy (*Acc*), taking T_a, *RH*, *ANR*, and *PI* as the input variables and v_s as the output. From this perspective, the BP method was proved to be a useful and promising alternative to the traditional methods for assessing tree physiological response using combinations of climatic data and physiological factor without knowing the complex mechanism involved in transpiration. Based on the results obtained in previous paper with pine and the ones obtained in this paper with Liquidambar, we concluded that the BP neural network methodology works in simulating SF for both a gymnosperm and an angiosperm.

Acknowledgements We thank the editors and two anonymous reviewers for their insightful comments. We are also grateful to Dr Huiming Wang and Fengting Yang for their kind assistance in analyzing meteorological data. Special thanks to Qianyanzhou Ecological Station, Chinese Academy of Science for offering the meteorological data and assistance in our field work.

Funding This work was financially supported by the National Natural Science Foundation of China (project No. 31260172) and the Country Scholarship of China (CSC No. 201408360046).

Data and code availability The datasets generated and/or analyzed during the current study are available in the Dryad repository, https://doi.org/10.5061/dryad.p5hqbzknx.

Declarations

Ethics approval Not applicable.

Consent to participate Not applicable.

Consent for publication Not applicable.

Competing interests The authors declare no competing interests.

References

Abrishami N, Sepaskhah AR, Shahrokhnia MH (2019) Estimating wheat and maize daily evapotranspiration using artificial neural network. Theor Appl Climatol 135(3–4):945–958

Adeloye AJ, Rustum R, Kariyama ID (2012) Neural computing modeling of the reference crop evapotranspiration. Environ Modell Softw 29:61–73

Aouade G, Ezzahar J, Amenzou N, Er-Raki S, Benkaddour A, Khabba S, Jarlan L (2016) Combining stable isotopes, Eddy Covariance system and meteorological measurements for partitioning evapotranspiration, of winter wheat, into soil evaporation and plant transpiration in a semi-arid region. Agr Water Manage 177:181–192

Asbjornsen H, Goldsmith GR, Alvarado-Barrientos MS, Rebel K, Osch FPV, Rietkerk M, Chen J, Gotsch S, Tobón C, Geissert DR,

Gómez-Tagle A, Vache K, Dawson TE (2011) Ecohydrological advances and applications in plant-water relations research: a review. J Plant Ecol 4:3–22

Bauerle WL, Whitlow TH, Pollock CR, Frongillo EA (2002) A laser-diode-based system for measuring sap flow by the heat-pulse method. Agr Forest Meteorol 110:275–284

Berdanier AB, Clark JS (2018) Tree water balance drives temperate forest responses to drought. Ecology 99:2506–2514

Bréda N, Granier A (1996) Intra- and interannual variations of transpiration, leaf area index and radial growth of a sessile oak stand (*Quercus petraea*). Ann Sci for 53(2–3):521–536

Bréda N, Huc R, Granier A, Dreye E (2006) Temperate forest trees and stands under severe drought: a review of ecophysiological responses, adaptation processes and long-term consequences. Ann Forest Sci 63:625–644

Brito P, Lorenzo JR, Gonzalez-Rodriguez AM, Morales D, Wieser G, Jimenez MS (2015) Canopy transpiration of a semi arid *Pinus canariensis* forest at a treeline ecotone in two hydrologically contrasting years. Agr Forest Meteorol 201:120–127

Buckley TN, Turnbull TL, Adams MA (2012) Simple models for stomatal conductance derived from a process model: cross-validation against sap flux data. Plant Cell Environ 35(9):1647–1662

Calder IR, Narayanswamy MN, Srinivasalu NV, Darling WG, Lardner AJ (1986) Investigation into the use of deuterium as a tracer for measuring transpiration from eucalypts. J Hydrol 84:345–351

Cavender-Bares J, Sack L, Savage J (2007) Atmospheric and soil drought reduce nocturnal conductance in live oaks. Tree Physiol 27:611–620

Chang X, Zhao W, He Z (2014) Radial pattern of sap flow and response to microclimate and soil moisture in Qinghai spruce (*Picea crassifolia*) in the upper Heihe River Basin of arid northwestern China. Agr Forest Meteorol 187(1):14–21

Chen DY, Wang YK, Liu SY, Wei XG, Wang X (2014) Response of relative sap flow to meteorological factors under different soil moisture conditions in rainfed jujube (*Ziziphus jujuba* Mill.) plantations in semiarid Northwest China. Agr Water Manage 136:23–33

Chen H, Huang JJH, McBean E (2020) Partitioning of daily evapotranspiration using a modified shuttleworthwallace model, random forest and support vector regression, for a cabbage farmland. Agr Water Manage 228:105923

Chirino E, Bellot J, Sánchez J (2011) Daily sap flow rate as an indicator of drought avoidance mechanisms in five Mediterranean perennial species in semi-arid southeastern Spain. Trees 25(4):593–606

Deutscher J, Kupec P, Dundek P, Holík L, Machala M, Urban J (2016) Diurnal dynamics of streamflow in an upland forested microwatershed during short precipitation-free periods is altered by tree sap flow. Hydrol Process 30:2042–2049

Dixon M, Grace J (1984) Effects of wind on the transpiration of young trees. Ann Bot 53:811–819

D'Odorico P, Gonsamo A, Gough CM, Bohrer G, Morison J, Wilkinson M, Hanson PJ, Gianelle D, Fuentes JD, Buchmann N (2015) The match and mismatch between photosynthesis and land surfacephenology of deciduous forests. Agr Forest Meteorol 214–215:25–38

Dragoni D, Lakso AN, Piccioni RM (2005) Transpiration of apple trees in a humid climate using heat pulse sap flow gauges calibrated with whole-canopy gas exchange chambers. Agr Forest Meteorol 130(1):85–94

Du S, Wang Y, Kume T, Zhang J, Otsuki K, Yamanaka N, Liu G (2011) Sapflow characteristics and climatic responses in three forest species in the semiarid Loess Plateau region of China. Agr Forest Meteorol 151(1):1–10

Dzikiti S, Verreynne SJ, Stuckens J, Strever A, Verstraeten WW, Swennen R, Theron KI, Coppin P (2011) Seasonal variation in canopy reflectance and its application to determine the water status and water use by citrus trees in the WesternCape, South Africa. Agr Forest Meteorol 151(8):1035–1044

Evaristo J, McDonnell JJ, Scholl MA, Bruijnzeel LA, Chun KP (2016) Insights into plant water uptake from xylem-water isotope measurements in two tropical catchments with contrasting moisture conditions. Hydrol Process 30:3210–3227

Faris H, Mirjalili S, Aljarah I (2019) Automatic selection of hidden neurons and weights in neural networks using grey wolf optimizer based on a hybrid encoding scheme. Int J Mach Learn Cyb 10(10):2901–2920

Fatichi S, Pappas C (2017) Constrained variability of modeled T: ET ratio across biomes. Geophys Res Lett 44:6795–6803

Fernandes TJG, Campo ADD, García-Bartual R, González-Sanchis M (2015) Coupling daily transpiration modelling with forest management in a semiarid pine plantation. iForest 9:38–48

Garcia-Santos G (2011) Transpiration in a subtropical ridge-top cloud forest. J Hydrol 462:42–52

Garrity SR, Bohrer G, Maurer KD, Mueller KL, Vogel CS, Curtis PS (2011) A comparison of multiple phenology data sources for estimating seasonal transitions in deciduous forest carbon exchange. Agr Forest Meteorol 151:1741–1752

Gharun M, Turnbull TL, Henry J, Adams MA (2015) Mapping spatial and temporal variation in tree water use with an elevation model and gridded temperature data. Agr Forest Meteorol 200:249-257

Ghimire CP, Lubczynski MW, Bruijnzeel LA, Chayarro-Rincon D (2014) Transpiration and canopy conductance of two contrasting forest types in the Lesser Himalaya of Central Nepal. Agr Forest Meteorol 197:76–90

Granier A (1987) Evaluation of transpiration in a Douglas-fir stands by means of sap flow measurements. Tree Physiol 3:309–320

Gonsamo A, Chen JM, D'Odorico P (2013) Deriving land surface phenology indicators from CO_2 eddy covariance measurements. Ecol Indic 29:203–207

González-Altozano P, Pave EW, Oncins JA, Doltra J (2008) CohenM, Paço T, Massai R, Castel JR (2008) Comparative assessment of five methods of determining sap flow in peach trees. Agr Water Manage 95(5):503–515

Grossiord C, Sevanto S, Dawson TE, Adams HD, Collins AD, Dickman LT, Newman BD, Stockton EA, McDowell NG (2017) Warming combined with more extreme precipitation regimes modifies the water sources used by trees. New Phytol 213:584–596

Huang JT, Zhou YX, Yin LH, Wenninger J, Zhang J, Hou GC, Zhang EY, Uhlenbrook S (2015) Climatic controls on sap flow dynamics and used water sources of *Salix psammophila* in a semi-arid environment in northwest China. Environ Earth Sci 73:289–301

Hudson IL (2010) Interdisciplinary approaches: towards new statistical methods for phenological studies. Clim Change 100(1):143–171

Humphrey GB, Gibbs MS, Dandy GC, Maier HR (2016) A hybrid approach to monthly streamflow forecasting: integrating hydrological model outputs into a Bayesian artificial neural network. J Hydrol 540:623–640

Han C, Chen N, Zhang CK, Liu YJ, Khan S, Lu KL, Li Y, Dong XX, Zhao CM (2019) Sap flow and responses to meteorological about the Larix principis-rupprechtii plantation in Gansu Xinlong mountain, northwestern China. Forest Ecol Manage 451:117519

Hayat M, Zha TS, Jia X, Iqbal S, Qian D, Bourque CPA, Khan A, Tian Y, Bai YJ, Liu P, Yang RZ (2020) A multiple-temporal scale analysis of biophysical control of sap flow in Salix psammophila growing in a semiarid shrub land ecosystem of northwest China. Agr Forest Meteorol 288–289:107985

Jeong SJ, Schimel D, Frankenberg C, Drewry DT, Fisher JB, Verma M, Berry JA, Lee JE, Joiner J (2017) Application of satellite solar-induced chlorophyll fluorescence to understanding large-scale variations in vegetation phenology and function over northern high latitude forests. Remote Sens Environ 190:178–187

Juhász Á, Sepsi P, Nagy Z, Tőkei L, Hrotkó K (2013) Water consumption of sweet cherry trees estimated by sap flow measurement. Sci Hortic 164:41–49

Kallarackal J, Otieno DO, Reineking B, Jung EY, Schmidt MWT, Granier A, Tenhunen JD (2013) Functional convergence in water use of trees from different geographical regions: a meta-analysis. Trees-Struct Func 27:787–799

Kalma SJ, Thorburn PJ, Dunn GM (1998) A comparison of heat pulse and deuterium tracing techniques for estimating sap flow in Eucalyptus grandis trees. Tree Physiol 18(10):697–705

Kirikoshi H, Nakano T (2011) Sap flow velocity of deciduous broad-leaved trees in urban area and its dependence on environmental factors. Clim Biosph 11:31–40

Konings AG, Williams AP, Gentine P (2017) Sensitivity of grassland productivity to aridity controlled by stomatal and xylem regulation. Nat Geosci 10:284–288

Kume T, Komatsu H, Kuraji K, Suzuki M (2008) Less than 20-min time lags between transpiration and stem sap flow in emergent trees in a Bornean tropical rainforest. Agr Forest Meteorol 148:1181–1189

Kume T, Laplace S, Komatsu H, Chu CR (2015) Transpiration in response to wind speed: can apparent leaf-type differences between conifer and broadleaf trees be a practical indicator? Trees 29(2):605–612

Li HT, Xiang L, Xia J, Lin YM, Liang T (2006) Applying the heat dissipation technique to study the sap flow of *Pinus elliottii* in the Red Earth Area of subtropical China. Sci Silvae Sin 42(10):31–38

Liu X, Kang S, Li F (2009) Simulation of artificial neural network model for trunk sap flow of Pyrus pyrifolia and its comparison with multiple-linear regression. Agr Water Manage 96(6):939–945

Liu CW, Du TS, Li FS, Kang SZ, Li SE, Tong L (2012) Trunk sap flow characteristics during two growth stages of apple tree and its relationships with affecting factors in an arid region of northwest China. Agr Water Manage 104:193–202

Liu X, Zhang B, Zhuang JY, Han C, Zhai L, Zhao WR, Zhang JC (2017) The Relationship between Sap Flow Density and Environmental Factors in the Yangtze River Delta Region of China. Forests 8(3):74

Marino G, Pallozzi E, Cocozza C, Tognetti R, Giovannelli A, Cantinid C, Centritto M (2014) Assessing gas exchange, sap flow and water relations using tree canopy spectral reflectance indices in irrigated and rainfed *Olea europaea* L. Environ Exp Bot 99(3):43–52

McCarthy HR, Pataki DE (2010) Drivers of variability in water use of native and non-native urban trees in the greater Los Angeles area. Urban Ecosyst 13:393–414

McNaughton KG, Jarvis PG (1983) Predicting effects of vegetation changes on transpiration and evaporation. In: Kozlowski TT (ed) Water deficits and plant growth, vol 6. Academic Press, New York, pp 1–47

Miner GL, Hamn JM, Kluitenberg GJ (2017) A heat-pulse method for measuring sap flow in corn and sunflower using 3D-printed sensor bodies and low-cost electronics. Agr Forest Meteorol 246:86–97

Monje O, Bingham GE, Carman JG, Campbell WF, Salisbury FB, Eames BK, Sytchev V, Levinskikh MA, Podolsky I (2000) Canopy photosynthesis and transpiration in micro-gravity: gas exchange measurements aboard Mir. Adv Space Res 26(2):303–306

Monteith JL (1997) Evaporation, evapotranspiration and climatic data. J Hydrol 190(1):167–168

Moore GW, Cleverly JR, Owens MK (2008) Nocturnal transpiration in riparian Tamarix thickets authenticated by sap flux, eddy covariance and leaf gas exchange measurements. Tree Physiol 28(4):521–528

Nourani V, Kalantari O (2010) An integrated artificial neural network for spatiotemporal modeling of rainfall runoff-sediment processes. Environ Eng Sci 27:411–422

Nourani V, Ejlali RG, Alami MT (2011) Spatiotemporal groundwater level forecasting in coastal aquifers by hybrid artificial neural network-Geostatistics Model: a case study. Environ Eng Sci 28(3):217–230

Nadal-Sala D, Sabaté S, Sánchez-Costa E, Poblador S, Sabater F, Carlos G (2017) Growth and water use performance of four co-occurring riparian tree species in a Mediterranean riparian forest. Forest Ecol Manage 396:132–142

Navarro A, Portillo-Estrada M, Arriga N, Vanbeveren SPP, Ceulemans R (2018) Genotypic variation in transpiration of coppiced poplar during the third rotation of a short-rotation bio-energy culture. GCB Bioenergy 10(8):592–607

Obrist D, Verburg PSJ, Young MH, Coleman JS, Schorran DE, Arnone IIIJA (2003) Quantifying the effects of phenology on ecosystem evapotranspiration in planted grassland mesocosms using Eco-CELL technology. Agr Forest Meteorol 118:173–183

O'brien JJ, Oberbauer SF, Clark DB (2004) Whole tree xylem sap flow responses to multiple environmental variables in a wet tropical forest. Plant Cell Environ 27:551–567

Oguntunde PG, van de Giesen NC, Vlek PLG, Eggers H (2004) Water flux in a Cashew Orchard during a wet-to-dry transition period: analysis of sap flow and eddy correlation Measurements. Earth Interact 8(15):1–17

O'Grady AP, Worledge D, Battaglia M (2008) Constraints on transpiration of *Eucalyptus globulus* in southern Tasmania, Australia. Agr Forest Meteorol 148:453–465

Paudel I, Naor A, Gal Y, Cohen S (2015) Simulating nectarine tree transpiration and dynamic water storage from responses of leaf conductance to light and sap flow to stem water potential and vapor pressure deficit. Tree Physiol 35(4):425–438

Pfautsch S, Bleby TM, Rennenberg H, Adams MA (2010) Sap flow measurements reveal influence of temperature and stand structure on water use of *Eucalyptus regnans* forests. Forest Ecol Manage 259:1190–1199

Prieto I, Kikvidze Z, Pugnaire FI (2010) Hydraulic lift: soil processes and transpiration in the Mediterranean leguminous shrub *Retama sphaerocarpa* (L.) Boiss. Plant Soil 329:447–456

Rabbel I, Diekkruger B, Voigt H, Neuwirth B (2016) Comparing ΔTmax determination approaches for Granier-based sapflow estimations. Sensors 16:2042

Saugier B, Granier A, Pontailler JY, Dufrêne E, Baldocchi DD (1997) Transpiration of a boreal pine forest measured by branch bag, sap flow and micrometeorological methods. Tree Physiol 17(8–9):511–519

Telander AC, Slesak RA, D'Amatoa AW, Palik BJ, Brooks KN, Lenhart CF (2015) Sap flow of black ash in wetland forests of northern Minnesota, USA: Hydrologic implications of tree mortality due to emerald ash borer. Agr Forest Meteorol 206:4–11

Tie Q, Hu HC, Tian FQ, Guan HD, Lin H (2017) Environmental and physiological controls on sap flow in a subhumid mountainous catchment in North China. Agr Forest Meteorol 240–241:46–57

Tu J, Wei XH, Huang BB, Fan HB, Jian MF, Li W (2019) Improvement of sap flow estimation by including phenological index and time-lag effect in back-propagation neural network models. Agr Forest Meteorol 276–277:107608

Tu J, Liu QJ, Wu JP (2021) Recognition of dominant driving factors behind sap flow of *Liquidambar formosana* based on back-propagation neural network method. Dryad. [Dataset]. 10.5061/dryad.p5hqbzknx

Vandegehuchte MW, Steppe K (2013) Sap-flux density measurement methods: working principles and applicability. Funct Plant Biol 40:213–223

Vandegehuchte MW, Burgess SSO, Downey A, Steppe K (2015) Influence of stem temperature changes on heat pulse sap flux density measurements. Tree Physiol 35:346–353

Venturin AZ, Guimarães CM, de Sousa EF, Filho JAM, Rodrigues WP, de SerrazineAraujo Í, Bressan-Smith R, Marciano CR, Campostrini E (2020) Using a crop water stress index based on a sap flow method to estimate water status in conilon coffee plants. Agr Water Manage 241:106343

Wang Q, Wang S, Huang Y (2008) Comparisons of litterfall, litter decomposition and nutrient return in a monoculture *Cunninghamia lanceolata* and a mixed stand in southern China. Forest Ecol Manage 255:1210–1218

Wang HM, Sun W, Zu YG, Wang WJ (2011) Complexity and its integrative effects of the time lags of environment factors affecting *Larix gmelinii* stem sap flow. J Appl Ecol 22:3109–3116

Wang XF, Liu JF, Sun YY, Li K, Zhang CH (2017) Sap flow characteristics of three afforestation species during the wet and dry seasons in a dry–hot valley in Southwest China. J Forest Res 28:51–62

Whitley R, Taylor D, Macinnis-Ng C, Zeppel M, Yunusa I, O'Grady A, Froend R, Medlyn B, Eamus D (2013) Developing an empirical model of canopy water flux describing the common response of transpiration to solar radiation and VPD across five contrasting woodlands and forests. Hydrol Process 27(8):1133–1146

Wieser G, Grams TEE, Matyssek R, Walter O, Gruber A (2015) Soil warming increased whole-tree water use of *Pinus cembra* at the treeline in the Central Tyrolean Alps. Tree Physiol 35:279–288

Wilson KB, Hanson PJ, Mulholland PJ, Baldocchi DD, Wullschleger SD (2001) A comparison of methods for determining forest evapotranspiration and itscomponents: sap-flow, soil water budget, eddy covariance and catchmentwater balance. Agr Forest Meteorol 106(2):153–168

Windt CW, Blümler P (2015) A portable NMR sensor to measure dynamic changes in the amount of water in living stems or fruit and its potential to measure sap flow. Tree Physiol 35:366–375

Wu YZ, Zhang YK, An J, Liu QJ, Lang Y (2018) Sap flow of black locust in response to environmental factors in two soils developed from different parent materials in the lithoid mountainous area of North China. Trees 32:675–688

Xu SQ, Yu ZB, Ji XB, Sudicky EA (2017) Comparing three models to estimate transpiration of desert shrubs. J Hydrol 550:603–615

Zanetti SS, Sousa EF, Oliveira VPS, Almeida FT, Bernardo S (2007) Estimating evapotranspiration using artificial neural network and minimum climatological data. J Irrig Drain Eng 133(2):83–89

Zapater M, Hossann C, Breda N, Brechet C, Bonal D, Granier A (2011) Evidence of hydraulic lift in a young beech and oak mixed forest using ^{18}O soil water labelling. Trees Struct Funct 68:433–442

Zha TS, Qian D, Jia X, Bai YJ, Tian Y, Bourque CPA, Ma JY, Feng W, Wu B, Peltola HL (2017) Soil moisture control of sap-flow response to biophysical factors in a desert-shrub species, Artemisia ordosica. Biogeosci 14(19):4533–4544

Zhang RF, Xu XL, Liu MX, Zhang YH, Xu CH, Yi RZ, Luo W, Soulsby C (2019) Hysteresis in sap flow and its controlling mechanisms for a deciduous broad-leaved tree species in a humid karst region. Sci China Earth Sci 62:1744–1755

Authors and Affiliations

Jie Tu[1] · Qijing Liu[2] · Jianping Wu[3]

Qijing Liu
liuqijing@gmail.com

Jianping Wu
jianping.wu@ynu.edu.cn

[1] School of Civil Engineering and Architecture, East China Jiao Tong University, Nanchang 330013, China

[2] College of Forestry, Beijing Forestry University, Beijing 100803, China

[3] Yunnan Key Laboratory of Plant Reproductive Adaption and Evolutionary Ecology, Yunnan University, Kunming 650500, China